0026-895X/05/6705-1600–1611$20.00
MOLECULAR PHARMACOLOGY
Copyright © 2005 The American Society for Pharmacology and Experimental Therapeutics
Mol Pharmacol 67:1600–1611, 2005

Vol. 67, No. 5
8839/1198140
Printed in U.S.A.

Amino Acids Critical for Substrate Affinity of Rat Organic Cation Transporter 1 Line the Substrate Binding Region in a Model Derived from the Tertiary Structure of Lactose Permease

Christian Popp, Valentin Gorboulev, Thomas D. Müller, Dmitry Gorbunov, Natalia Shatskaya, and Hermann Koepsell

Institute of Anatomy and Cell Biology (C.P., V.G., D.G., N.S., H.K.) and Institute of Physiological Chemistry (T.D.M.), University of Würzburg, Würzburg, Germany

Received October 29, 2004; accepted January 19, 2005

ABSTRACT

To identify functionally relevant amino acids in the rat organic cation transporter 1 (rOCT1), 18 consecutive amino acids in the presumed fourth transmembrane α helix (TMH) were mutated and functionally characterized after expression in *Xenopus laevis* oocytes. After mutation of three amino acids on successive turns of the α helix, K_m values for tetraethylammonium (TEA) and/or 1-methyl-4-phenylpyridinium (MPP) were decreased. After replacement of Trp218 by tyrosine (W218Y) and Tyr222 by leucine (Y222L), the K_m values for both TEA and MPP were decreased. In mutants Y222F and T226A, only the K_m values for TEA and MPP were decreased, respectively. The data suggest that amino acids Trp218 and Tyr222 participate in the binding of both TEA and MPP, whereas Thr226 is only involved in the binding of MPP. Using the crystal structure of the lactose permease LacY from *Escherichia coli* that belongs to the same major facilitator superfamily as rOCT1, we modeled the tertiary structure of the presumed 12 transmembrane α helices. The validity of the model was suggested because seven amino acids that have been shown to participate in the binding of cations by mutagenesis experiments [fourth TMH Trp218, Tyr222, and Thr226 (this work); 10th TMH Ala443, Leu447, and Gln448 (companion work in this issue of *Molecular Pharmacology*); 11th TMH Asp475 (previous report)] are located in one region surrounding a large cleft that opens to the intracellular side. The dimensions of TEA in comparison with the interacting amino acids in the modeled cleft suggest that more than one TEA molecule can bind in parallel to the modeled conformation of the transporter.

The *SLC22* transporter family, a member of the major facilitator superfamily (MFS), comprises polyspecific transporters with 12 presumed transmembrane α helices (TMH) for organic cations, organic anions, and zwitterions (Koepsell et al., 2003; Koepsell, 2004). Three subtypes of polyspecific organic cation transporters have been identified (*SLC22A1–3* or OCT1–3). These transporters are critically involved in the elimination of cationic drugs and metabolic waste products in liver and kidney. OCT1 is mainly expressed in liver, where it is localized at the sinusoidal membrane of the hepatocytes (Gründemann et al., 1994; Gorboulev et al., 1997; Meyer-Wentrup et al., 1998). It mediates the first step in biliary secretion of organic cations (i.e., their uptake into hepatocytes). Because the transporters OCT1 to -3 can transport cations in both directions (Busch et al., 1996; Budiman et al., 2000; Koepsell et al., 2003), OCT1 is supposed to be responsible also for the release of organic cations across the sinusoidal membrane into the blood. Using nontransported inhibitors in combination with giant-patch method, we determined ligand affinities of the outwardly and inwardly oriented conformations of the substrate binding region of rat OCT2 (Volk et al., 2003). These data suggest that the binding region of rOCT2 comprises overlapping binding sites for different substrates that differentially alter their affinity during reorientation. This interpretation was supported by the observation

This study was supported by the Deutsche Forschungsgemeinschaft grant SFB 487/A4.

C.P. and V.G. contributed equally to the work.

Article, publication date, and citation information can be found at http://molpharm.aspetjournals.org.
doi:10.1124/mol.104.008839.

ABBREVIATIONS: MFS, major facilitator superfamily; TMH, transmembrane α-helix; OCT, organic cation transporter; LacY, lactose permease Y; TEA, tetraethylammonium; MPP, 1-methyl-4-phenylpyridinium; PBS, phosphate-buffered saline; TPeA, tetrapentylammonium; PCR, polymerase chain reaction; PDB, Protein Data Bank; m, mouse; r, rat; h, human; MOPS, 3-(*N*-morpholino)propanesulfonic acid.

that the mutation of aspartate 475 to glutamate in the binding region of rOCT1 led to a drastic increase in affinity for some substrates and competitive inhibitors but did not influence the affinity of another substrate (Gorboulev et al., 1999).

For the understanding of drug transport and for the design of drugs with optimized biodistribution and excretion, it is important to elucidate the structure of the substrate binding regions of polyspecific transporters of the *SLC22* family, how various substrates bind to these regions, whether more than one substrate can bind simultaneously, and how substrate binding initiates the translocation process. In the end, these questions can only be solved by the crystallization of ligand-transporter complexes in combination with functional characterization of point mutations of critical residues.

In recent years, the functional effects of many individual point mutations on transport activity and/or substrate affinity of transporters of the *SLC22* family have been described previously (Koepsell et al., 2003; Koepsell and Endou, 2004). It turned out that mutations in several of the presumed 12 membrane-spanning α helices (TMHs 1, 2, 4, 7, 8, and 11) in the large extracellular loop and in the large intracellular loop lead to functional changes such as differential affinity changes for various substrates. Considering the possibility that part of these changes are caused by long-range effects on the conformation of the substrate binding region, we reasoned that indirect effects were much less probable if amino acids with specific effects on substrate affinity could be identified in neighboring positions within the secondary structure (e.g., on one side of an α-helix). For this reason, we carried out a systematic mutational screening of the presumed fourth TMH of rOCT1. We measured transport activity for two different substrates in mutants of 18 consecutive amino acids and investigated 9 of these amino acids in more detail. The fourth TMH was selected because this TMH contains several amino acids on one side of the presumed α helix that are conserved within the three OCT subtypes but not in the closely related organic anion transporters. We obtained data indicating that three amino acids in neighboring positions on one side of the presumed fourth TMH participate in substrate binding.

The three-dimensional structures of three members of the major facilitator superfamily, the oxalate transporter OxlT from *Oxalobacter formigenes* (Hirai et al., 2002), the lactose permease LacY *Escherichia coli* (Abramson et al., 2003), and the glycerol-3-phosphate transporter GlpT from *E. coli* (Huang et al., 2003) have recently been reported. These transporters had similar structures containing large clefts that were crystallized in an orientation directed to the cytosol. For LacY, it was shown that this cleft contained the substrate binding site. On the basis of the structure of LacY, we modeled the presumed TMHs of rOCT1 with a large cleft similar to LacY. The validity of this model was supported by mutagenesis. Seven amino acids whose mutations increased substrate affinities are located in one region surrounding the large cleft and are accessible from the aqueous phase.

Materials and Methods

Site-Directed Mutagenesis. Point mutations were introduced in rOCT1 (Gründemann et al., 1994) by polymerase chain reaction (PCR) applying the overlap extension method (Ho et al., 1989). The oligonucletides used as flanking primers were the following: 5′-CCA TCT ATG TGG GCA TCG-3′ (rOCT1, nucleotides 138–155) and 5′-ACA GCA GGA AGA GGA AGG-3′ (rOCT1, nucleotides 872–855). The PCR amplificates were digested with AccI and NheI, and gel-purified fragments were ligated into wild-type rOCT1/pRSSP vector (Busch et al., 1996) that was cut with the same restriction endonucleases. The fragments introduced into rOCT1/pRSSP were sequenced to confirm the presence of the desired mutations and to exclude PCR errors. For immunodetection, the FLAG epitope (DYKDDDDK) was added to the C terminus of rOCT1 wild type and mutants, using the overlap extension PCR procedure and using the rOCT1-FLAG primers (with underlined FLAG sequences) 5′-GAC TAC AAG GAT GAC GAT GAC AAG TGA CAG GGA TGC TG-3′ (forward) and 5′-CTT GTC ATC GTC ATC CTT GTA GTC AGT ACT TGA GGA CTT G-3′ (reverse). The PCR amplificates were digested with Eco130I and BglII, gel-purified, and substituted for the respective fragment of rOCT1 in the rOCT1/pRSSP vector.

cRNA Transcription and Expression in *Xenopus laevis* Oocytes. For injection into *X. laevis* oocytes, m7G(5′)ppp(5′)G-capped sense cRNAs were transcribed in vitro using the mMESSAGE mMACHINE kit (Ambion, Huntingdon, Cambridgeshire, UK). The pRSSP vectors containing rOCT1 wild-type or rOCT1 mutants (Busch et al., 1996) were linearized with MluI, and cRNAs were synthesized using SP6 RNA polymerase. cRNA concentrations were estimated from ethidium bromide-stained agarose gels using polynucleotide marker as standards (Gründemann and Koepsell, 1994). Stage V to VI oocytes were defolliculated with collagenase A (Veyhl et al., 1993) and stored for several hours in Ori buffer [5 mM MOPS-NaOH, pH 7.4, 100 mM NaCl, 3 mM KCl, 2 mM $CaCl_2$, and 1 mM $MgCl_2$] supplemented with 50 mg/l gentamicin. The oocytes were injected with 10 ng of the respective cRNA in 50 nl of H_2O. For comparison in parallel experiments, cRNAs of wild-type and mutant rOCT1 were injected within 3 h into oocytes from the same batch. For transporter expression, the oocytes were incubated for 3 to 5 days at 16°C in Ori buffer supplemented with 50 mg/l gentamicin.

Enrichment of Plasma Membranes of *X. laevis* Oocytes. Three days after incubation of cRNA-injected oocytes or noninjected oocytes in Ori buffer, a plasma membrane-enriched fraction was prepared at 4°C as described previously (Geering et al., 1989). Oocytes were homogenized in homogenization buffer (10 mM HEPES, pH 7.9, 83 mM NaCl, 1 mM $MgCl_2$, 1 mM phenylmethylsulfonyl fluoride, 0.05 ng/ml leupeptin, and 10 mM benzamidine), centrifuged for 10 min at 1000*g*, and the supernatant was carefully removed leaving lipids behind. The pellet was suspended in homogenization buffer, centrifuged for 10 min at 1000*g*, and the supernatant was collected. Both supernatants were combined and centrifuged for 20 min at 10,000*g*. The pellet was suspended in homogenization buffer and recentrifuged for 20 min at 10,000*g*. The obtained pellet was enriched in plasma membranes as demonstrated previously by marker enzymes (Geering et al., 1989) and by immunodetection of the expressed sodium-D-glucose cotransporter SGLT1 (Valentin et al., 2000). Protein was quantified according to the method of Bradford using bovine serum albumin as standard (Bradford, 1976).

Western Blotting. Enriched plasma membrane fractions from *X. laevis* oocytes were incubated for 30 min at 37°C in 60 mM Tris HCl, pH 6.8, 100 mM dithiothreitol, 2% (w/v) SDS, and 7% (v/v) glycerol and separated by SDS-polyacrylamide gel electrophoresis as described previously (Valentin et al., 2000). Proteins were transferred to polyvinyl difluoride membrane and incubated with affinity-purified polyclonal antibody raised against the large extracellular loop of rOCT1 as described earlier (Meyer-Wentrup et al., 1998). Bound peroxidase-conjugated secondary antibody (goat anti-rabbit IgG) was visualized by enhanced chemiluminescence (ECL system; Amersham Buchler, Braunschweig, Germany). Prestained molecular weight marker BenchMark (Invitrogen, Carlsbad, CA) was used to determine apparent molecular masses.

Immunocytochemistry. Oocytes were treated as described previously (Wolff et al., 2001). On day 3 after injection, oocytes were incubated for 5 min in 200 mM potassium aspartate, manually

devitellinized, and then fixed overnight at −20°C in 80% (v/v) methanol and 20% (v/v) dimethyl sulfoxide. The permeabilized oocytes were rehydrated, washed in phosphate-buffered saline (PBS), and incubated at 4°C for 12 h with mouse anti-FLAG M2 IgG monoclonal antibody (Sigma Chemie, Deisenhofen, Germany) (dilution, 1:2000) in the presence of 10% (v/v) goat serum (Sigma Chemie). After washing in PBS, oocytes were incubated for 1 h at room temperature with secondary Alexa 546 goat anti-mouse IgG antibody (Molecular Probes, Eugene, OR) (dilution, 1:200). Oocytes were washed in PBS, postfixed for 30 min at room temperature in 3.7% (v/v) paraformaldehyde, and embedded in acrylamide (Technovit 7100; Heraeus Kulzer, Wehrheim, Germany). Embedded oocytes were cut into 5-μm sections and analyzed by epifluorescence microscopy.

Tracer Uptake Measurements. For uptake measurements, the oocytes were incubated at 19°C for 30 min in Ori buffer containing [^{14}C]TEA, [^{3}H]MPP, [^{14}C]guanidine, [^{3}H]histamine, or [^{3}H]serotonin. Oocytes were then added to ice-cold Ori buffer plus 100 μM quinine, washed in the same buffer, solubilized in 5% (w/v) SDS, and analyzed for radioactivity. Uptake in oocytes expressing rOCT1 wild type or mutants was corrected for uptake by noninjected oocytes. TEA and MPP uptake by noninjected oocytes was identical with the uptake by oocytes expressing transporter in the presence of 100 μM quinine, an inhibitor of OCTs.

Calculation and Statistics. Uptake in oocytes expressing rOCT1 wild -type or mutants was calculated from 7 to 10 oocytes and corrected for nonspecific uptake measured in 7 to 10 noninjected control oocytes. K_m and V_{max} values were calculated by fitting the Michaelis-Menten equation to the corrected uptake measured with 7 to 10 different substrate concentrations. IC_{50} values were calculated from individual experiments by fitting the Hill equation for multisite inhibition to uptake rates in the presence of 7 to 10 different inhibitor concentrations. Considering the large variations of expression levels and regulatory state between different batches of oocytes, uptake by rOCT1 mutants was always measured in parallel with uptake by rOCT1 wild type in oocytes from the same batch and within 3 h. The experiments reported in the present work were performed over a period of 3 years. During this time, considerable variability of expressed uptake rates and some variability of the K_m values of individual transporters were observed. For example, for TEA uptake by rOCT1 wild type, the V_{max} values varied between 60 and 420 pmol × oocyte^{-1} h^{-1}, whereas the K_m values varied between 55 and 133 μM. The large differences in V_{max} values can be explained by differences in expression level between oocyte batches. The observed differences in K_m values are supposed to be caused by oocyte batch-dependent differences in membrane potential or transporter regulation (Mehrens et al., 2000; Arndt et al., 2001). To enable a comparison of mutants, we expressed uptake, K_m, V_{max}, and IC_{50} values as percentages of the respective values for rOCT1 wild type obtained in parallel measurements. Data are presented as mean ± S.E.M. values obtained from three to six independent experiments. The paired two-sided Student's t test was used to assess the statistical significance of differences between 1) uptake rates of TEA or MPP by mutants versus wild type measured in parallel (Table 1); 2) relative uptake rates of TEA versus MPP by individual mutants in parallel experiments (Table 1); and 3) K_m or V_{max} values for mutants versus wild-type rOCT1 from parallel measurements (Table 2 and Fig. 4). Unpaired two-sided Student's t test was used to compare K_m or V_{max} values for TEA versus MPP of individual mutants that were obtained from measurements that were not strictly performed in parallel (Fig. 4), or to compare K_m or V_{max} values between different mutants from measurements that were not strictly performed in parallel (Fig. 4). In the experimental series shown in Fig. 3, we performed an analysis of variance followed by Tukey's test to assess the differences between relative uptake rates of five different substrates by various mutants.

Modeling the Tertiary Structure of rOCT1. We used the tertiary structure of lactose permease LacY from *E. coli*, which was recently crystallized (PDB entry 1PV6) (Abramson et al., 2003), to model the tertiary structure of the putative TMHs of rOCT1. The putative TMHs of rOCT1 indicated in Fig. 6 were predicted using the software TMHMM (http://www.cbs.dtu.dk/services/TMHMM/). The putative TMHs of rOCT1 were then aligned to the respective helices of LacY using CLUSTALW or Bestfit of the software package GCG Wisconsin (Accelrys, San Diego, CA). The model was built by replacing the residues of LacY with the corresponding residues of rOCT1 using the software package Quanta2000 (Accelrys). Close contacts were removed by rotamer searches for the affected side chains. Further steric clashes were eliminated by using energy minimization

TABLE 1

Comparison of uptake rates of TEA and MPP by rOCT1 mutants in which one of the amino acids between positions 212 and 229 was exchanged

rOCT1 wild type and the indicated mutants of rOCT1 were expressed in oocytes. The uptake of 10 μM [^{14}C]TEA or 0.1 μM [^{3}H]MPP over 30 min was corrected for nonspecific uptake by noninjected oocytes and expressed as percentage of the uptake by rOCT1 wild type, which was measured in parallel. Mean ± S.E.M. values from three to six experiments are presented.

Mutants	Uptake	
	TEA	MPP
	%	
M212L	97 ± 10	98 ± 7
V213G	28 ± 9*	51 ± 12
S214G	42 ± 1***	44 ± 12*
×K215Q	0 ± 0.1***	0.1 ± 0.1***
×K215R	0.2 ± 0.1***	1.6 ± 0.5***
G216A	8.7 ± 1.9***†	24 ± 2***
S217G	118 ± 28	128 ± 21
W218F	28 ± 5**†	133 ± 43
V219L	69 ± 9	90 ± 20
S220I	26 ± 4**†	53 ± 3*
G221A	42 ± 9*	57 ± 9*
Y222F	78 ± 9	122 ± 30
T223I	64 ± 5*	75 ± 24
L224V	17 ± 6**	34 ± 10*
I225G	83 ± 9	92 ± 7
T226A	76 ± 4*†	90 ± 3
×E227Q	0.1 ± 0.1***	0.1 ± 0.2***
×E227D	0 ± 0.1***	0 ± 0.1***
F228I	89 ± 10	88 ± 12
V229A	32 ± 13*	54 ± 8*
×V229L	0.2 ± 0.1***	0.1 ± 0.1***

* $P < 0.05$; ** $P < 0.01$; *** $P < 0.001$, statistical significance of differences between wild-type vs. mutants.

† $P < 0.05$, statistical significance of difference between TEA vs. MPP in individual mutants.

×, inactive mutant.

TABLE 2

K_m and V_{max} for TEA and MPP uptake by rOCT1 mutated at single amino acids within the presumed fourth TMH

Parallel measurements were performed with noninjected oocytes, oocytes expressing rOCT1 wild type, and oocytes expressing rOCT1 mutants. Uptake rates in oocytes expressing rOCT1 wild type or mutants were corrected for uptake in noninjected oocytes. The Michaelis-Menten equation was fitted to the data of individual experiments. K_m and V_{max} values calculated for mutants are presented as percentages of values that were measured in parallel for rOCT1 wild type. Mean ± S.E.M. values of three independent experiments are shown.

Mutants	K_m		V_{max}	
	TEA	MPP	TEA	MPP
V213G	432 ± 18*†	279 ± 43*	66 ± 14	69 ± 8
G216A	90 ± 23	158 ± 62	8 ± 3**	17 ± 6**
W218F	81 ± 13	86 ± 19	46 ± 14†	96 ± 10
S220I	193 ± 48	212 ± 56	41 ± 10*	67 ± 10
Y222F	31 ± 8*†	112 ± 22	29 ± 3*	57 ± 11*
L224V	43 ± 17	53 ± 24	10 ± 4**	16 ± 3*
T226A	64 ± 18	33 ± 4*	48 ± 8	46 ± 3**
V229A	313 ± 68*	137 ± 34	56 ± 12	57 ± 15

* $P < 0.05$; ** $P < 0.01$, statistical significance of differences between wild-type and mutants.

† $P < 0.05$, statistical significance between TEA and MPP uptake.

procedures via the CHARMM forcefield (Accelrys). The backbone geometry was retained by defining distance restraints for the backbone atoms mimicking the hydrogen bonding pattern of LacY. These distance restraints obeyed a nuclear Overhauser effect-like constraints potential with upper and lower distance boundaries; target distance was set to 2.1 Å, lower boundary was set to 1.9 Å between the amide proton and the carbonyl oxygen, and the upper boundary for this atom pair was set to 2.4 Å. At sites in which nonglycine or nonprolines residues of the LacY template were exchanged to glycine or prolines of rOCT1, no distance restraints were used to allow for an adaptation of the backbone conformation. The distances were weighted with a rather high force constant of 250 kcal $mol^{-1}Å^{-2}$ in the initial refinement steps (first 100 minimization steps), and the force constant was then gradually lowered (100 minimization steps per round, lowering the force constant by 50 kcal $mol^{-1}Å^{-2}$ each round, final force constant = 50 kcal $mol^{-1}Å^{-2}$) to allow for more conformational freedom during the final steps of energy minimization within CHARMM. The overall fold was maintained also by a set of distance restraints that were defined between the N- and C-terminal "ends" of the TMHs. These distance were also used with upper and lower boundaries; however, the boundaries were set to ±25% of the respective distance to allow for smaller changes in the packing of the TMHs. After several rounds of energy minimization, a short molecular-dynamic simulation in vacuo (10 ps) was performed with the backbone, and overall geometry was restrained as indicated above using the CHARMM force field of the software package Quanta2000. These maneuvers led to low energies for geometry and van der Waals interaction terms. The large loops of rOCT1 were excluded from the modeling because LacY lacks a corresponding structure (loop between TMHs 1 and 2) or exhibits low structural similarity (loop between TMHs 6 and 7).

Materials. [^{14}C]TEA (1.9 GBq/mmol), [^{3}H]MPP (3.1 TBq/mmol), and [^{14}C]guanidine (2.0 GBq/mmol) were obtained from Biotrend. [^{3}H]Histamine (1.9 TBq/mmol) and [^{3}H]serotonin (0.7 TBq/mmol) were purchased from Amersham Biosciences Europe GmbH (Freiburg, Germany), and tetrapentylammonium (TPeA) from Sigma Chemie. The other chemicals were obtained as described earlier (Meyer-Wentrup et al., 1998; Arndt et al., 2001).

Results

Mutation Scanning of Amino Acids Comprising the Presumed Fourth Transmembrane α Helix of rOCT1. To investigate the role of the presumed fourth TMH for cation selectivity of rOCT1, we replaced each amino acid between positions 212 and 229 with similar amino acids or with amino acids from corresponding positions in other members of the *SLC22* transporter family (Koepsell et al., 1999). We expressed the mutants in oocytes and measured the uptake rates of 10 μM [^{14}C]TEA and of 0.1 μM [^{3}H]MPP in comparison with wild type (Table 1). No significant uptake of TEA and MPP was expressed by the mutants K215Q, K215R, E227Q, E227D, and V229L. When Val229 was replaced by alanine, a less bulky amino acid than leucine, relatively high uptake rates of TEA (32% of wild type) and MPP (54% of wild type) were expressed.

To investigate translation and membrane insertion for mutants that did not express the uptake of TEA (K215R, E227D, and V229L), we performed Western blots with enriched plasma membranes and investigated the localization of the transporters in intact oocytes. To enable the immunocytochemical detection in acrylamide-embedded oocytes, we appended a FLAG-tag to the C terminus of wild-type and mutant transporters. With FLAG-tagged wild-type rOCT1, a similar uptake rate of 10 μM [^{14}C]TEA was expressed compared with nonmodified wild type. No significant uptake of TEA was expressed with the FLAG-tagged mutants K215R, E227D, and V229L as observed with the unmodified mutants (data not shown). Western blots with preparations of enriched plasma membranes obtained by differential centrifugation revealed similar staining for FLAG-tagged wild-type and mutants. The Western blot in Fig. 1a was developed with a previously described affinity-purified antibody against the large extracellular loop of rOCT1 (Meyer-Wentrup et al., 1998). The antibody reacted with two polypeptide bands with apparent molecular masses of ~50 and ~70 kDa and showed a less intense reaction with an ~45-kDa protein. The intensity of this band varied between different experiments (Gorboulev et al., 1999). The upper band was absent after deglycosylation (V. Gorboulev, M. Elfeber, and H. Koepsell, unpublished data). Together, these data indicate that the mutants are translated and glycosylated similar to rOCT1 wild type.

Figure 1b shows immunostaining of oocytes expressing FLAG-tagged wild type and FLAG-tagged mutants K215R, E227D, and V229L using a monoclonal antibody against the

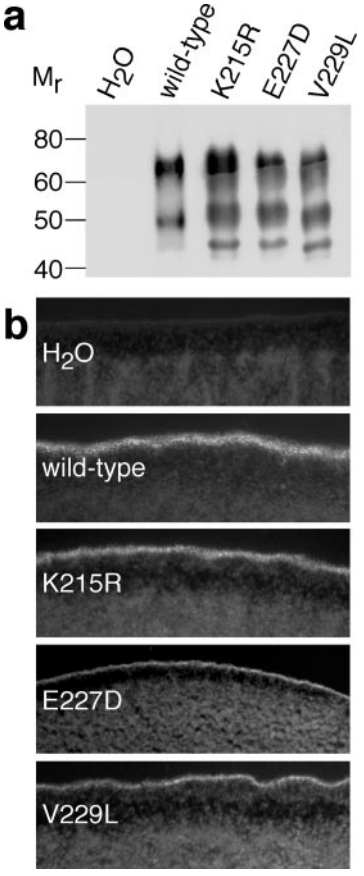

Fig. 1. Demonstration of translation, membrane incorporation, and plasma membrane association of inactive mutants. rOCT1 wild-type and the indicated mutants, all tagged with a FLAG-epitope at the C terminus, were expressed in *X. laevis* oocytes. a, Western blot on plasma membrane enriched subcellular fractions isolated from oocytes injected with water or respective cRNAs. The blots were stained with affinity-purified antibody directed against the large extracellular loop of rOCT1. b, location of expressed rOCT1 wild type and mutants at the plasma membrane. The oocytes were fixed, permeabilized, and stained with an antibody directed against the FLAG epitope. The data show that mutants K215R, E227D, and V229L are translated into protein and transported to the plasma membrane.

FLAG epitope. Immunostaining at the plasma membrane in oocytes expressing rOCT1 wild type and the mutants indicates translation and membrane insertion. By fluorescence microscopy and confocal laser scanning microscopy, we were not able to differentiate staining at the plasma membrane from vesicles just beneath it (data not shown). For this reason and because the FLAG tag was attached to the intracellular C termini, the immunolocalization data do not exclude location in vesicles beneath the plasma membrane.

After replacing Gly216 with alanine, Trp218 with phenylalanine, Ser220 with isoleucine, or Thr226 with alanine, the uptake of 10 μM TEA was reduced to a greater extent than the uptake of 0.1 μM [^{3}H]MPP (Table 1; $P < 0.05$ for difference). This indicates changes in substrate selectivity.[1] Trends toward altered substrate selectivity were observed for the mutants V213G, Y222F, L224V, and V229A (Table 1). To confirm these trends, and to determine whether the different changes in transport rates of TEA versus MPP are caused by altered affinities or maximal transport velocities, concentration dependence of TEA and MPP uptake was measured (Table 2). In the mutant V213G, the K_m values for both TEA and MPP were increased significantly compared with wild type, indicating a decrease in substrate affinity. The increase in K_m value for TEA was significantly higher than the increase in K_m value for MPP. This explains the higher transport activity for MPP versus TEA measured in Table 1. After mutating Gly216 to alanine, the K_m values for TEA and MPP were not changed, whereas the V_{max} values for both substrates were reduced. The V_{max} for TEA seemed to be reduced to a greater extent than the V_{max} for MPP. This may explain the higher uptake of MPP versus TEA in Table 1. After replacing Trp218 by phenylalanine, the V_{max} value for TEA was halved, whereas the V_{max} value for MPP was not changed ($P < 0.05$ for different effects on V_{max}). Substrate concentration-dependence of mutant S220I revealed a statistically significant reduction of the V_{max} for TEA and a trend toward a less-pronounced reduction of V_{max} for MPP. This can explain the lower uptake of TEA versus MPP in Table 1. In mutant Y222F, the K_m for TEA was significantly lower compared with wild type ($P < 0.05$), whereas the K_m for MPP was not changed. In addition, the V_{max} values for TEA and MPP were decreased. Because the data indicate an increase in affinity for TEA, which may be considered as gain of function, we investigated mutant Y222F in more detail and exchanged Tyr222 with two other amino acids (see below). After mutation of Leu224 to valine, the V_{max} values for TEA and MPP were significantly decreased, and a trend for a decrease in K_m values was observed. After exchange of Thr226 with alanine, the K_m and V_{max} values for MPP were significantly decreased, whereas the K_m and V_{max} values for TEA showed only a trend for a decrease. Because this mutation also led to an affinity increase, it was further characterized (see below). Finally, in the V229A mutant, the K_m value for TEA was significantly increased versus wild type, whereas the K_m for MPP was not changed significantly.

Further Characterization of Mutants of Conserved Amino Acids Localized on One Side of the Presumed Fourth TMH. Secondary structure prediction suggests a TMH between amino acids 212 and 229 (Koepsell et al., 1999). An α-helical wheel representation of that TMH shows that the two mutations with significantly increased substrate affinity (Y222F and T226A) affect amino acids on the same side of this α helix (Fig. 2). They belong to a group of five neighboring amino acids on this side of the presumed fourth TMH (Lys215, Trp218, Tyr222, Thr226, and Val229) that are conserved in organic cation transporters but not in organic anion transporters (Koepsell et al., 1999). We further characterized the function of these amino acids by additional transport measurements and in additional mutations (W218Y, W218L, and Y222L). To identify putative changes in substrate selectivity in point mutation, we measured the uptake of 10 μM [^{14}C]TEA, 0.5 μM [^{3}H]MPP, 200 μM [^{14}C]guanidine, 30 μM [^{3}H]histamine, or 2.5 μM [^{3}H]serotonin in the mutants K215Q, K215R, W218F, W218Y, W218L, Y222F, Y222L, T226A, V229L, and V229A in comparison to rOCT1 wild type. Note that the substrate concentrations used in these experiments were more than eight times lower than the respective K_m values in rOCT1 wild type (Arndt et al., 2001; Koepsell et al., 2003); therefore, changes in the uptake rates may reflect changes in affinity, maximal transport velocity, or both.

Mutants K215Q, K215R, and V229L, which did not mediate the uptake of TEA and MPP (Table 1), were also not able to mediate uptake of guanidine, histamine, or serotonin (data not shown). With mutant V229A, uptake rates for TEA, MPP, guanidine, histamine, and serotonin were approximately 50% of the respective uptake rates observed with rOCT1 wild type. The substrate selectivity of this mutant was not different from wild type (data not shown). Mutants W218F, W218Y, and W218L exhibit significantly different substrate selectivities between each other and compared with rOCT1

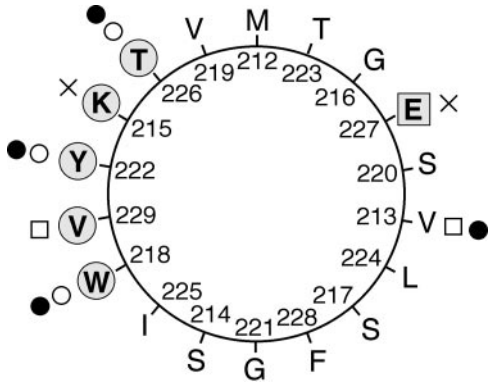

Fig. 2. Synopsis of mutational analysis of the presumed 4th TMH of rOCT1 shown as a helical wheel. TMH4 is assumed to be a standard α helix with 3.6 residues/helical turn, and each residue is plotted every 100° around the center of the circle starting with M212. Circles, amino acids that are conserved in the OCTs but not in the organic anion transporters (in mOCT3 and rOCT3 Tyr222 is replaced with phenylalanine). □, Glu227 is conserved throughout all transporters of the *SLC22* family. ×, mutants in these positions were inactive. ○, mutants in these positions revealed decreased K_m values. □, mutants in these positions had increased K_m values. ●, mutants in these positions exhibited changed selectivity. Mutants of the unlabeled amino acids did not show significant changes of functional properties.

[1] We use the term "change in substrate selectivity" in a broad sense. It means that the relation between uptake rates of two (or more) substrates is changed under at least one experimental condition. Such a "change in substrate selectivity" can show up at low substrate concentrations, at high substrate concentrations, or under both conditions. It may be caused by substrate-specific changes in turnover (V_{max}) and/or K_m. Changes in substrate selectivity of mutants relative to wild type indicate substrate-specific changes of uptake rates. Such changes do not necessarily alter the rank order of uptake rates between substrates.

wild type (Fig. 3). In all three Trp218 mutants, the smallest changes of uptake rates compared with wild type were observed for MPP. In W218F and W218Y, the uptake rates for MPP were similar to wild type but were reduced by approximately 80% in W218L. Significant changes in substrate selectivity were also observed after mutations of Tyr222 and Thr226 (Fig. 3). Substrate selectivity was changed in mutant Y222L but not in Y222F. Unique substrate selectivity different from wild type was also obtained in the T226A mutant.

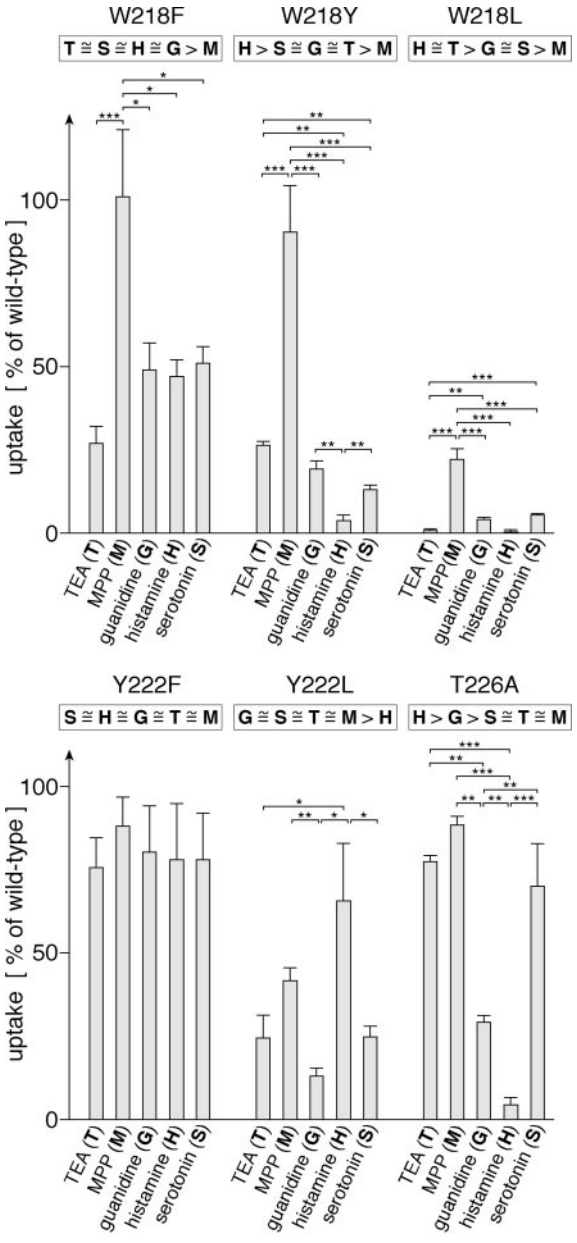

Fig. 3. Changes of substrate selectivity after mutation of amino acids on one side of the presumed fourth TMH. Noninjected oocytes, oocytes injected with cRNAs of rOCT1 wild type, and oocytes injected with cRNAs of mutants were incubated for 3 days. For transport measurements, the oocytes were incubated for 30 min with 10 μM [^{14}C]TEA, 0.5 μM [^{3}H]MPP, 0.2 mM [^{14}C]guanidine, 30 μM [^{3}H]histamine, or 2.5 μM [^{3}H]serotonin, and the uptake of radioactivity was measured. The uptake by oocytes expressing rOCT1 mutant was corrected for uptake by noninjected oocytes and normalized to the corrected uptake by rOCT1 wild type measured in parallel. Mean values ± S.E.M. of three to four individual experiments in which the five different substrates were measured in parallel are presented. ⋆, $P < 0.05$; ⋆⋆, $P < 0.01$; ⋆⋆⋆, $P < 0.001$, statistical significance of differences between relative uptake rates of different substrates (ANOVA with post hoc Tukey's test). The indicated rank order of substrates describes the magnitude of changes in transport rates in the mutants compared with wild type. The data show unaltered substrate selectivity of Y222F and changed substrate selectivities of W218F, W218Y, W218L, Y222L, and Thr226.

When changes in substrate selectivity are identified by uptake measurements of different substrates using a single fixed concentration of each substrate as in Fig. 3, changes in affinity cannot be distinguished from changes of maximal transport rate. Changes in K_m values may thus be overlooked if they are combined with opposite changes of V_{max}. For example, after replacement of Tyr222 with phenylalanine, the uptake rates of 10 μM TEA and 0.5 μM MPP were similar to those of wild type (Fig. 3), although the K_m and V_{max} values for TEA were significantly decreased compared with wild type (Table 2). When the affinity of a substrate is increased after a point mutation, we reasoned that the respective amino acid may be involved in substrate binding because it is not very likely that an increase of affinity is caused by an indirect effect on the structure. It is obvious that point mutations in a substrate binding site can lead to a decrease in substrate affinity; however, there is a high probability that mutations outside of a binding site induce structural changes that have the same effect.

A significant decrease of the K_m value for TEA was observed in mutant Y222F, and a significant decrease of the K_m value for MPP in mutant T226A was also observed (Table 2). Thus, Tyr222 and Thr226 are probably localized in the substrate binding region of rOCT1. To understand the functional role of Trp218, which is localized next to Tyr222 on the α helix, and to further investigate the functional role of Tyr222, we compared substrate dependence of TEA uptake versus MPP uptake after the replacement of Trp218 by phenylalanine, tyrosine, and leucine and after replacement of Tyr222 by phenylalanine and leucine. Figure 4 shows the apparent K_m and V_{max} values of these mutants. As described above, the K_m values for TEA and MPP and the V_{max} value for MPP were not changed by the W218F mutation, whereas the V_{max} value for TEA uptake was decreased by 50% (Table 2 and Fig. 4). When Trp218 was replaced with tyrosine, the function of rOCT1 was changed in a different way: K_m and V_{max} values for both TEA and MPP were decreased significantly compared with wild type. Note that the additional hydroxyl group in W218Y compared with W218F leads to a higher affinity for both MPP and TEA. Replacement of Trp218 with leucine resulted in a drastic decrease of the affinity for TEA, whereas the affinity for MPP was not changed. At variance, after the exchange of this amino acid, the V_{max} values for TEA and MPP uptake were decreased by similar degrees. In summary, point mutations in position 218 can lead to changes in substrate affinity and transport rates that are independent from each other. The changes in substrate affinity can be specific for certain substrates and can include an increase of substrate affinity. The data suggest that in addition to Tyr222 and Thr226, Trp218 is localized within the substrate binding region of rOCT1 and that Trp218 can interact with both TEA and MPP. The K_m independent changes of V_{max} values observed in mutants W218F and W218L suggest that Trp218 participates in conformational changes during substrate translocation.

Different effects on the affinity of TEA and MPP were also observed when Tyr222 was replaced by phenylalanine or

leucine. As described above, the K_m value for TEA uptake in Y222F was significantly decreased, whereas the K_m value for MPP uptake remained unchanged, suggesting that Tyr222 is located in the substrate binding region (Table 2 and Fig. 4). When Tyr222 was replaced with leucine, the K_m values for TEA and MPP decreased by similar degrees (Fig. 4; TEA by 53%, MPP by 65%). In parallel, the V_{max} values for TEA and MPP were decreased by 91 and 90%, respectively. The functional properties of Y222L support the interpretation that Tyr222 is localized in the substrate region of rOCT1.

To further characterize mutants Y222F and Y222L, we investigated the effect of these mutations on two high-affinity inhibitors, cyanine 863, and the quaternary ammonium salt TPeA. Previous mutagenesis showed that TPeA binds to the substrate binding region of rOCT1 (Gorboulev et al., 1999). In the Y222F mutant, the IC_{50} value for inhibition of TEA (10 μM) uptake by cyanine 863 was not significantly different from rOCT1 wild type (data not shown). However, the IC_{50} value for inhibition of TEA uptake by TPeA was largely decreased (Fig. 5). For inhibition of TEA uptake by TPeA, we determined IC_{50} values (mean ± S.E.M., $n = 3$) of 1.0 ± 0.2 μM (rOCT1 wild type, Hill coefficient 0.58 ± 0.05) and 0.05 ± 0.02 μM (Y222F, Hill coefficient 0.66 ± 0.10) ($P <$ 0.05 for difference between IC_{50} values). The IC_{50} value for TPeA inhibition of TEA uptake by the Y222L mutant was not significantly different from wild type (IC_{50} = 2.2 ± 0.7, n = 3, Hill coefficient 1.0 ± 0.1). Taken together, the data confirm the interpretation that Tyr222 is located within the substrate binding region of rOCT1 and suggest that Tyr222 interacts with TEA, MPP, and TPeA.

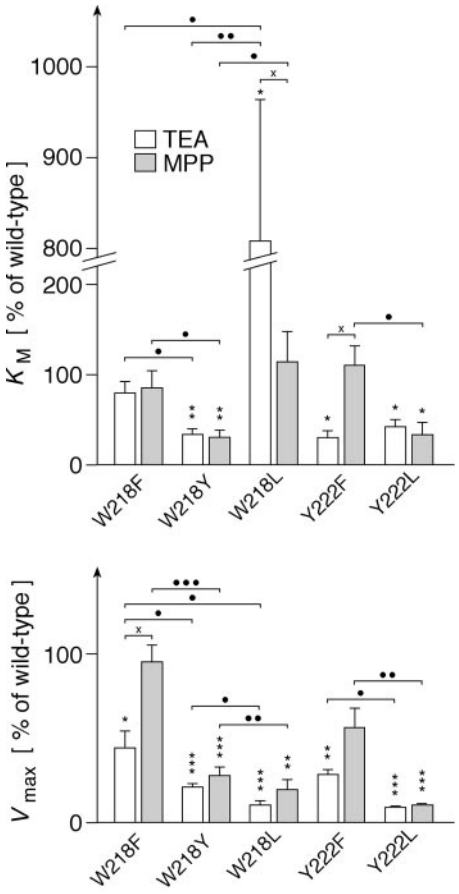

Fig. 4. Concentration dependence of TEA and MPP transport by rOCT1 upon mutation of Trp218 and Tyr222. In each experiment, noninjected oocytes, oocytes injected with rOCT1 wild-type cRNA, and oocytes injected with mutant cRNAs were incubated for 3 days, and uptake of [^{14}C]TEA or [^{3}H]MPP was measured at various concentrations of the respective substrate. Uptake in oocytes expressing rOCT1 wild type or mutants were corrected for the uptake measured in noninjected oocytes. K_m and V_{max} values were calculated and normalized to the K_m and V_{max} values of rOCT1 wild type measured in the respective experiment. Mean values ± S.E.M. of three to four individual experiments are presented. ⋆, $P < 0.05$; ⋆⋆, $P < 0.01$; ⋆⋆⋆, $P < 0.001$, statistical significance of differences between wild type and mutants. ●, $P < 0.05$; ●●, $P < 0.01$; ●●●, $P < 0.001$, statistical significance for the difference of K_m or V_{max} values between different mutants. ×, $P < 0.05$, statistical significance of difference of K_m value for TEA versus MPP or of V_{max} value for TEA versus MPP. The data show that K_m values for TEA and MPP were decreased in parallel or separately when Trp218 and Tyr222 were replaced with different amino acids.

In this study, we estimated the affinity of rOCT1 wild type and mutants for TEA and MPP by calculating apparent K_m values from substrate concentration-dependence of uptake. Experiments in the accompanying article show that the K_m values for TEA or MPP uptake by rOCT1 wild type and two rOCT1 mutants with increased substrate affinity (rOCT1 L447Y/Q448E, rOCT1 A443I/L447Y/Q448E) were not significantly different from the IC_{50} values for inhibition of MPP (0.1 μM) uptake by TEA, or for the inhibition of TEA (10 μM) uptake by MPP (Gorboulev et al., 2005). In the present article, we compared K_m and IC_{50} values of additional mutants. We expressed the mutants W218F, W218Y, and W218L in parallel with rOCT1 wild type and measured both the apparent K_m values for substrate activation of TEA uptake and the IC_{50} values for inhibition of MPP (0.1 μM) uptake by TEA. From three independent experiments, the following K_m versus IC_{50} values were determined: rOCT1 wild type, 94 ± 27 versus 122 ± 20 μM; W218F, 41 ± 6 versus 69 ± 23 μM; W218Y, 30 ± 5 versus 38 ± 6 μM; and W218L, 760 ± 149 versus 854 ± 90 μM. The Hill coefficients calculated from the inhibition experiments were not significantly different (rOCT1 wild type, 0.92 ± 0.13; W218F, 0.72 ± 0.14; W218Y, 0.72 ± 0.05; and W218L, 1.07 ± 0.18). In conclusion, the comparisons between K_m and IC_{50} values for TEA and MPP performed so far suggest that the same binding steps of TEA and MPP are characterized by both methods.

Modeling the Structure of the Substrate Binding Pocket of rOCT1. The lactose permease LacY of *E. coli* was crystallized recently, and the tertiary structure was determined at 3.3-Å resolution (Abramson et al., 2003). Because LacY and the organic cation transporters belong to the MFS, we tried to model the tertiary structure of the presumed

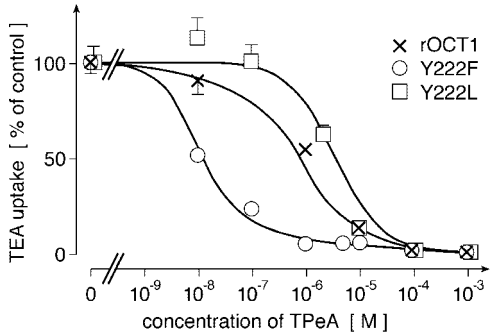

Fig. 5. Inhibition of TEA uptake by TPeA in rOCT1 wild type and mutants Y222F and Y222L. Uptake of 10 μM [^{14}C]TEA was measured in the presence of the indicated concentrations of TPeA. A representative experiment of three is shown. The Hill equation was fitted to the data. The IC_{50} value of TPeA was largely decreased in the Y222F mutant.

transmembrane α helices of rOCT1 on the basis of the LacY structure. To test the validity of the structural model we analyzed whether the amino acids that have been located within the substrate binding site by mutagenesis experiments line the substrate binding pocket predicted by the model. By mutagenesis experiments, three amino acids on one side of the fourth TMD (Trp218, Tyr222, and Thr226; see above), three amino acids in the 10th TMD (Ala443, Leu447, and Gln448) (Gorboulev et al., 2005), and one amino acid in the 11th TMD (Asp475) (Gorboulev et al., 1999) were assigned to the substrate binding region of rOCT1. Figure 6 shows an alignment of the presumed TMHs of the three OCT subtypes from rat and human with the respective helices of the LacY. For the sequences shown in Fig. 6, 12.4% of the amino acids were identical between rOCT1 and LacY, whereas 28.8% of the amino acids were similar. Considering the sequences of the three OCT subtypes from human and rat together, 18.5% of amino acids were identical, and 37% of the amino acids were similar between at least one of the OCTs and LacY. By analogy to the tertiary structure of LacY

```
          1                                helix 1                                52
rOCT1     MPTVDDVLEQ VGEFGWFQKQ AFLLLCLISA SLAPIYVGIV FLGFTPGHY- CQN.......
hOCT1     MPTVDDILEQ VGESGWFQKQ AFLILCLLSA AFAPICVGIV FLGFTPDHH- CQS.......
rOCT2     MSTVDDILEH IGEFHLFQKQ TFFLLALLSG AFTPIYVGIV FLGFTPDHH- CWS.......
hOCT2   MPTTVDDVLEH GGEFHFFQKQ MFFLLALLSA TFAPIYVGIV FLGFTPDHR- CRS.......
rOCT3     MPTFDQALRK AGEFGRFQRR VFLLLCLTGV TFAFLFVGVV FLGSQPDYYW CRG.......
hOCT3     MPSFDEALQR VGEFGRFQRR VFLLLCLTGV TFAFLFVGVV FLGTQPDHYW CRG.......
LacY                    MYYLKNT NFWMFGLFFF FYFFIMGAYF PFFPIWLHDI N.........

              146          helix 2                          helix 3          201
rOCT1     ....AWKVDL FQSCVNLGFF LGSLVVGYIA DRFGRKLCLL VTTLVTSVSG VLTAVAPDYT
hOCT1     ....SWKLDL FQSCLNAGFF FGSLGVGYFA DRFGRKLCLL GTVLVNAVSG VLMAFSPNYM
rOCT2     ....SWMLDL FQSVVNVGFF IGAMMIGYLA DRFGRKFCLL VTILINAISG ALMAISPNYA
hOCT2     ....SWMLDL FQSSVNVGFF IGSMSIGYIA DRFGRKLCLL TTVLINAAAG VLMAISPTYT
rOCT3     ....AWMLDL TQAILNLGFL AGAFTLGYAA DRYGRLIVYL ISCFGVGITG VVVAFAPNFS
hOCT3     ....AWMLDL TQAILNLGFL TGAFTLGYAA DRYGRIVIYL LSCLGVGVTG VVVAFAPNFP
LacY      ....KSDTGI IFAAISLFSL LFQPLFGLLS DKLGLRKYLL WIITGMLV-M FAPFFIFIFG

          202                    helix 4                    helix 5          251
rOCT1     SML------- --LFRLLQGM VSKGSWVSGY TLITEFVG-S GYRRTTAILY QMAFTVGLVG
hOCT1     SML------- --LFRLLQGL VSKGNWMAGY TLITEFVG-S GSRRTVAIMY QMAFTVGLVA
rOCT2     WML------- --VFRFLQGL VSKAGWLIGY ILITEFVG-L GYRRMVGICY QIAFTVGLLI
hOCT2     WML------- --IFRLIQGL VSKAGWLIGY ILITEFVG-R RYRRTVGIFY QVAYTVGLLV
rOCT3     VFV------- --IFRFLQGV FGKGAWMTCF VIVTEIVG-S KQRRIVGIVI QMFFTLGIII
hOCT3     VFV------- --IFRFLQGV FGKGTWMTCY VIVTEIVG-S KQRRIVGIVI QMFFTLGIII
LacY      PLLQYNILVG SIVGGIYLGF CFNAGAPAVE AFIEKVSRRS NFEFGRARMF GCVGWALGAS

          252          helix 6                    helix 7                    362
rOCT1     LAGVAYAIPD WRWLQLAVSL PTFLFLLYYW FV..... NLRKHTVILM YLWFSCAVLY
hOCT1     LTGLAYALPH WRWLQLAVSL PTFLFLLYYW CV..... RLRKRTFILM YLWFTDSVLY
rOCT2     LAGVAYVIPN WRWLQFAVTL PNFCFLLYFW CI..... QIRKHTLILM YNWFTSSVLY
hOCT2     LAGVAYALPH WRWLQFTVAL PNFFFLLYYW CI..... QIRKHTMILM YNWFTSSVLY
rOCT3     LPGIAYFTPS WQGIQLAISL PSFLFLLYYW VV..... QMRKCTLILM FAWFTSAVVY
hOCT3     LPGIAYFIPN WQGIQLAITL PSFLFLLYYW VV..... QMRKCTLILM FAWFTSAVVY
LacY      IVGIMFTINN QFVFWLGSGC ALILAVLLFF AK..... KLWFLSLYVI GVSCTYDVFD

          363          helix 8                    helix 9          415
rOCT1     QGLIMHVGA- ------TGAN LYLDFFYSSL VEFPAAFIIL VTIDRIGRIY PIAASNLVTG
hOCT1     QGLILHMGA- ------TSGN LYLDFLYSAL VEIPGAFIAL ITIDRVGRIY PMAMSNLLAG
rOCT2     QGLIMHMGL- ------AGDN IYLDFFYSAL VEFPAAFIII LTIDRVGRRY PWAVSNMVAG
hOCT2     QGLIMHMGL- ------AGDN IYLDFFYSAL VEFPAAFMII LTIDRIGRRY PWAASNMVAG
rOCT3     QGLVMRLGL- ------IGGN LYMDFFISGL VELPGALLIL LTIERLGRRL PFAASNIVAG
hOCT3     QGLVMRLGI- ------IGGN LYIDFFISGV VELPGALLIL LTIERLGRRL PFAASNIVAG
LacY      QQFANFFTSF FATGEQTRVF GYVTTMGELL NASIMFFAPL I-INRIGGKN ALLLAGTIMS

          416          helix 10                   helix 11         474
rOCT1     AACLLMIFIP HELH-WLNVT LACLGRMGAT IVLQMVCLVN AELYPTFIRN LGMMVCSALC
hOCT1     AACLVMIFIS PDLH-WLNII IMCVGRMGIT IAIQMICLVN AELYPTFVRN LGVMVCSSLC
rOCT2     AACLASVFIP DDLQ-WLKIT IACLGRMGIT MAYEMVCLVN AELYPTYIRN LGVLVCSSMC
hOCT2     AACLASVFIP GDLQ-WLKII ISCLGRMGIT MAYEIVCLVN AELYPTFIRN LGVHICSSMC
rOCT3     VSCLVTAFLP EGIP-WLRTT VATLGRLGIT MAFEIVYLVN SELYPTTLRN FGVSLCSGLC
hOCT3     VACLVTAFLP EGIA-WLRTT VATLGRLGIT MAFEIVYLVN SELYPTTLRN FGVSLCSGLC
LacY      VRIIGSSFAT SALEVVILKT LHMFEVPFLL VGCFKYITSQ FEVR--FSAT IYLVCFCFFK

          475                    helix 12                         530
rOCT1     DLGGIFTPFM VFRLMEVWQ- -ALPLILFGV LGLTAGAMTL LLPETKGVAL PETIEEAE...
hOCT1     DIGGIITPFI VFRLREVWQ- -ALPLILFAV LGLLAAGVTL LLPETKGVAL PETMKDAE...
rOCT2     DIGGIITPFL VYRLTDIWM- -EFPLVVFAV VGLVAGALVL LLPETKGKAL PETIEDAE...
hOCT2     DIGGIITPFL VYRLTNIWL- -ELPLMVFGV LGLVAGGLVL LLPETKGKAL PETIEEAE...
rOCT3     DFGGIIAPFL LFRLAAIWL- -ELPLIIFGI LASVCGGLVM LLPETKGIAL PETVEDVE...
hOCT3     DFGGIIAPFL LFRLAAVWL- -ELPLIIFGI LASICGGLVM LLPETKGIAL PETVDDVE...
LacY      QLAMIFMSVL AGNMYESIGF QGAYLVLGLV ALGFTLISVF TLSGPGPLSL LRRQVNEV...
```

Fig. 6. Amino acid alignment of the presumed TMHs of OCTs with the TMHs of LacY from *E. coli*. The three OCT subtypes from rat (rOCT1, rOCT2, and rOCT3) and human (hOCT1, hOCT2, hOCT3) were aligned with LacY. Amino acids that are identical between lactose permease and organic cation transporters are indicated in boldface, and similar amino acids are highlighted. Numbering is performed according to rOCT1 (Gründemann et al., 1994).

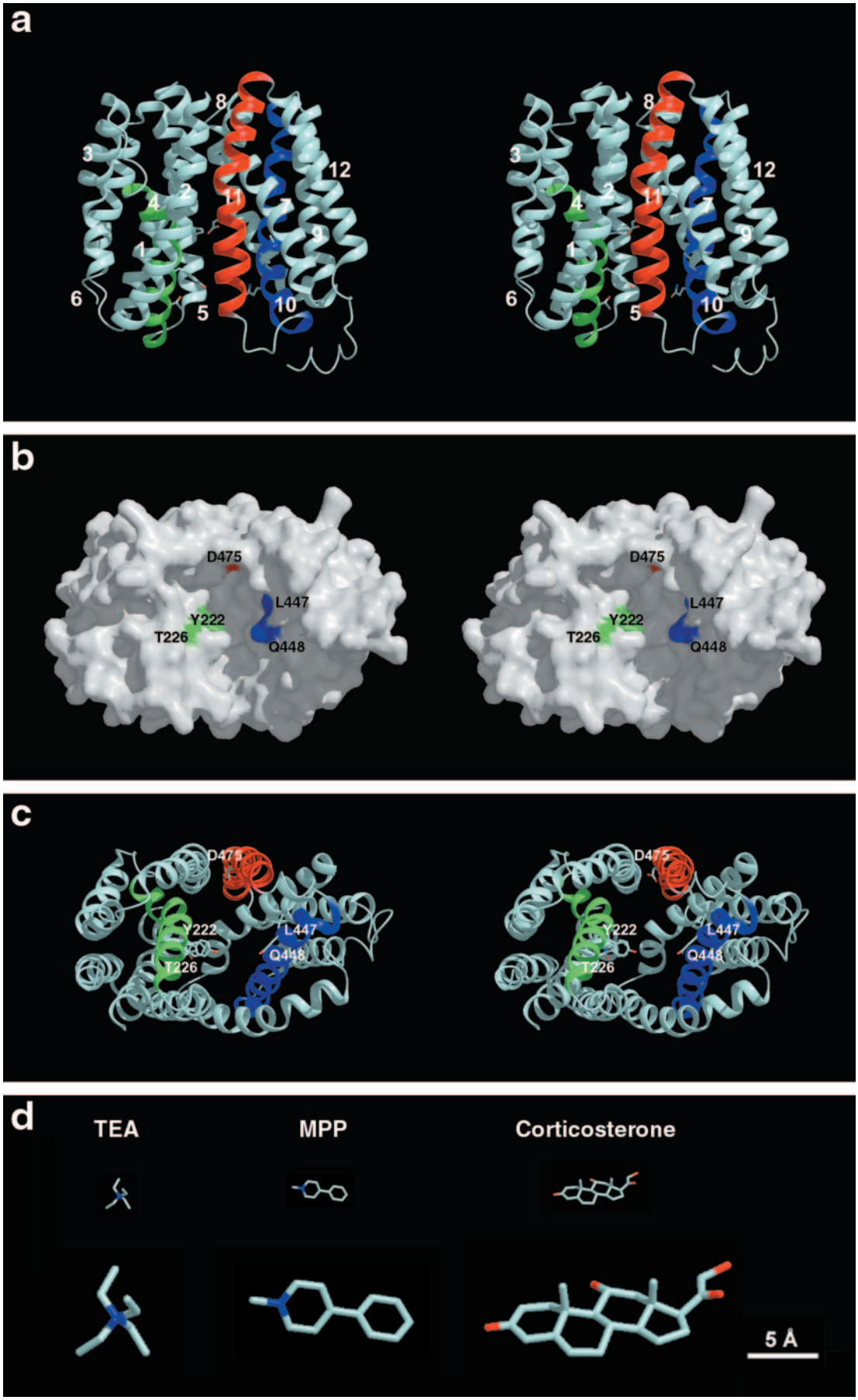
a
8
3
12
2
11
4
7
9
1
6
5
10
b
D475
L447
Y222
T226
Q448
c
D475
Y222
L447
Q448
T226
d
TEA
MPP
Corticosterone
5 Å

(Abramson et al., 2003) and two other transporters of the MFS superfamily, the oxalate transporter OxlT from *O. formigenes* (Hirai et al., 2002) and the glycerol-3-phosphate transporter GlpT from *E. coli* (Huang et al., 2003), the model in Fig. 7 shows a large cleft in rOCT1 that is accessible from the intracellular side of the membrane. The cleft in rOCT1 is formed by the 1st, 2nd, 4th, 5th, 7th, 8th, 10th, and 11th TMH (Fig. 7a). The model is strongly supported by our mutagenesis experiments, because all amino acids that have been identified to be involved in the substrate binding (4th TMH: Trp218, Tyr222, and Thr226; 10th TMH: Ala443, Leu447, and Gln448; 11th TMH, Asp475) are located in the large cleft of the modeled transporter and are accessible from the aqueous phase (Fig. 7, a–c). Note that these amino acids are located at a similar depth within the large cleft. They may be part of a substrate binding region surrounding the cleft. The cross-area of the cleft in this part is approximately 20×60 Å. The cleft has a depth of approximately 80 Å. The comparison of the modeled substrate binding region surrounding the cleft with the sizes of TEA, MPP, and corticosterone suggests that more than one of these compounds can bind at the same time.

Because similar high-resolution tertiary structures have been reported for LacY and GlpT (Abramson et al., 2003; Huang et al., 2003) and the amino acid similarity between these transporters is not larger than the similarity between rOCT1 and LacY, it is likely that the tertiary structure of rOCT1 is similar to both proteins. A comparison between the structures of LacY and GlpT showed that the transmembrane topology is highly conserved between these two transporters; a structural alignment yields a root mean square deviation of 4 Å if the Cα atoms of 382 equivalent residues are considered (PDB entry 1PW4 was used for GlpT, and PDB entry 1PV6 was used for LacY). Comparing the structural model of rOCT1 with to tertiary structure of GlpT, the Cα atoms of the seven residues within the substrate binding region of rOCT1 are within a distance of less than 4 Å compared with the respective residues of GlpT and exhibit similar side-chain orientations.

Discussion

The mutagenesis experiments presented in this article strongly suggest that the three amino acids Trp218, Tyr222, and Thr226 on succeeding turns of the presumed fourth TMH form part of the substrate binding region of rOCT1. Mutations in these amino acids resulted in significant decreases of K_m values for MPP and/or TEA. In mutants W218Y and Y222L, the K_m values were decreased for both TEA and MPP; in mutant Y222F, the K_m value for TEA was decreased; and in mutant Thr226, the K_m value for MPP was decreased. The data suggest that TEA and MPP bind to Trp218 and Tyr222 and that MPP binds also to Thr226. Ionic interaction of the positive charges in TEA and MPP with π-electrons of Trp218 and Tyr222 (Dougherty, 1996) and hydrophobic and van der Waals interactions with Trp218, Tyr222, and Thr226 may be involved. Trp218 is supposed to play a role in TEA translocation because in the W218F mutant, the V_{max} value for TEA was decreased, whereas the K_m value for TEA remained unchanged. Tyr222 may be important for the translocation of MPP because in the Y222F mutant, the V_{max} value for MPP was decreased, whereas the K_m value for MPP was not altered.

Mutation of other amino acids in the presumed fourth TMH drastically decreased transport activity (K215Q, K215R, E227Q, E227D, and V229L; see Table 1) or increased K_m value for TEA and changed substrate selectivity (V213G and V229A; see Table 2). These amino acids may be crucial for the tertiary structure of the substrate binding region. In mutant V213G, the K_m values for TEA and MPP were increased by different degrees, and in mutant V229A, the K_m value for TEA was increased, whereas the K_m value for MPP was not changed. Val213 is localized on the opposite side of the presumed fourth TMH compared with Trp218, Tyr222, and Thr226 (Fig. 2). Its replacement with alanine may change the position of the fourth TMH and thus the position of Trp218, Tyr222, and Thr226 (see model in Fig. 7, a and c). Val229 on the same side of the fourth TMH as Trp218, Tyr222, and Thr226 (Fig. 2) is located close to the transition between the fourth and fifth TMHs (Fig. 7c). After replacement of Val229 with leucine, this more bulky amino acid compared with valine or alanine may interact with the fifth TMH and thereby change the position of the fourth TMH that contains the above-described substrate binding domain.

The crystal structure of the lactose permease LacY from *E. coli* (Abramson et al., 2003) provided the possibility to model the tertiary structure of the TMHs of rOCT1. rOCT1 belongs to the same superfamily of transporters (MFS) as LacY (Koepsell et al., 2003) and shows 29% similar amino acids in the TMHs. We tested the validity of the structural rOCT1 model by evaluating the localization of seven amino acids that have been shown to be involved in substrate binding by mutagenesis experiments. Three amino acids on the presumed fourth TMH (Trp218, Tyr222, and Thr226) were identified above, three amino acids on the presumed 10th TMH (Ala443, Leu447, and Gln448) were identified in the accompanying article (Gorboulev et al., 2005), and one amino acid in the 11th TMH (Asp475) was identified earlier (Gorboulev et al., 1999). All seven amino acids fulfill the criterion that their exchange with an appropriate amino acid led to an increase of substrate affinity that was often combined with a change in substrate selectivity. Such a change of function is not likely to be induced by indirect effects. For Trp218, Tyr222, and Thr226, indirect effects can be virtually excluded as reason for the observed affinity changes in all three positions.

Fig. 7. Structure model of rOCT1. Modeling was performed using the tertiary structure of LacY (PDB entry 1PV6) from *E. coli.* a, stereo view of a ribbon presentation of the rOCT1 model. The individual TMHs are numbered. The 4th, 10th, and 11th TMHs are colored in green, blue, and red, respectively. Amino acid side chains on these TMHs that have been localized to the substrate binding region by mutagenesis experiments are depicted (Trp218, Tyr222, and Thr226 on the fourth TMH, Ala443, Leu447, and Gln448 on the 10th TMH, and Asp475 on the 11th TMH). b, stereo view of the van der Waals surface of the rOCT1 model (cytoplasmic view). In this orientation, only four of the above-mentioned seven amino acids are visible; however, all seven are located on the accessible surface of the binding region surrounding the cleft. c, ribbon representation of the rOCT1 model oriented as in b to show the location of all seven amino acids. The side chains of amino acids Trp218, Tyr222, Thr226, Ala443, Leu447, Gln448, and Asp475 are indicated. Numbering of amino acids Trp218 and Ala443 is omitted for sake of clarity. d, molecular structures of TEA, MPP, and corticosterone in two magnifications; the presentation of the top shows the size in respect to the model of rOCT1 in a to c; the bottom shows the structures in a larger representation. The bar is shown for the lower panel in d.

The high quality of our model of rOCT1 is strongly supported by the finding that all seven amino acids, which belong to the substrate binding region as judged from mutagenesis, are located within one structural epitope in the large cleft of the rOCT1 model and are in contact with the aqueous phase.

The positions of the seven amino acids in the modeled cleft of rOCT1 suggests that two or more substrates can bind in parallel to this conformation of the transporter. A decrease of the K_m value for TEA was observed after mutations of Asp475 in the 11th TMH (Gorboulev et al., 1999), of Trp218 or Tyr222 on successive turns of the fourth TMH, and after a combined mutation of Ala443, Leu447, and Gln448 in the 10th TMH (Gorboulev et al., 2005), and in our model, one TEA molecule cannot interact simultaneously with Asp475, Trp218, Tyr222, and an amino acid in the 10th TMH. Our mutagenesis experiments indicate that the binding sites for TEA in the proposed substrate binding region overlap with the binding sites for MPP, TPeA, and/or corticosterone. Note that in addition to TEA, 1) the affinity for MPP was increased in mutants of Trp218, of Tyr222, and in the triple mutant Ala443/Leu447/Gln448; 2) the affinity of corticosterone was increased after mutations of Ala443, Leu447, and/or Gln448; and 3) the affinity for TPeA was increased after mutations of Asp475 and Tyr222 (see above; Gorboulev et al., 1999, 2005).

Our interpretation that two or more substrates and/or inhibitors can bind at the same time is supported by data that suggest short-range allosteric interactions between ligands within the substrate binding region of rOCT1 (Gorboulev et al., 2005). After exchanging two amino acids in the substrate binding region (L447Y/Q448E), we observed a significantly higher affinity for the inhibition of TEA (10 μM) uptake by corticosterone compared with the inhibition of MPP (0.1 μM) uptake by corticosterone. These data suggest different short-range allosteric interactions between TEA and corticosterone versus MPP and corticosterone because of the following: 1) TEA, MPP, and corticosterone bind to the substrate binding region; 2) the differences in corticosterone affinity cannot be explained with different replacement of corticosterone by the two substrates; and 3) it is unlikely that the observed substrate effect on corticosterone affinity is caused by allosteric interaction between rOCT1 monomers because it was only observed after mutation of two amino acids in the substrate binding region.

The question arises whether simultaneous binding of more than one substrate molecule to the substrate binding region of rOCT1 is compatible with the observations that rOCT1 exhibits Michaelis-Menten type kinetics (Koepsell et al., 2003), that the IC_{50} values measured for TEA inhibition of MPP (0.1 μM) uptake expressed by rOCT1 and various mutants were similar to the K_m values for TEA (see above), and that mutations of amino acids at distant locations within the substrate region lead to decreases of K_m and IC_{50} values (see above). These observations could be reconciled if transport of TEA or MPP requires simultaneous or successive substrate binding to two or more binding sites within the large cleft and if the K_m and IC_{50} values reflect binding to more than one of these sites. In addition, it is possible that the outwardly directed conformation of the substrate binding region has a more tight structure that allows the simultaneous interaction of one TEA molecule with Asp475, Trp218, Tyr222, and one amino acid in the 10th TMH. In measuring the substrate concentration dependence of cation uptake by rOCT1 wild type and mutants, so far no sign for cooperativity has been detected. At variance, in some cases, we obtained Hill coefficients different from 1 for the inhibition of cation uptake (e.g., for inhibition of OCT1 wild type and Y222F mutant by TPeA, see Fig. 5). Ligand binding measurements with rOCT1 and mutants are required to prove simultaneous ligand binding and short-range allosteric interactions within the binding region. Molecular monitoring of structural changes within the substrate binding region may provide additional insights.

The proposed hypothesis that rOCT1 contains a large substrate binding region within a large cleft that can bind simultaneously several substrates and/or inhibitors is consistent with the crystal structure of the multidrug efflux pump AcrB from *E. coli* (Yu et al., 2003). AcrB is a polyspecific transporter like rOCT1; however, it has no structural similarity to rOCT1 and is energized by a proton gradient. It is interesting that crystal structures of AcrB-ligand complexes showed that three ligands bind simultaneously to a binding region of AcrB, that different ligands use a slightly different subset of AcrB residues for binding, and that the bound ligands interact with each other. At variance to AcrB, which contains a channel-like transmembrane path, the proposed LacY-like structure of rOCT1 implicates and functional data suggest that the large cleft in rOCT1 may be accessible either from the intracellular side of the plasma membrane or from the extracellular side of the plasma membrane (Volk et al., 2003). It is a challenge to determine the crystal structure of rOCT1 and resolve the transport mechanism.

References

Abramson J, Smirnova I, Kasho V, Verner G, Kaback HR, and Iwata S (2003) Structure and mechanism of the lactose permease of *Escherichia coli. Science (Wash DC)* **301:**610–615.

Arndt P, Volk C, Gorboulev V, Budiman T, Popp C, Ulzheimer-Teuber I, Akhoundova A, Koppatz S, Bamberg E, Nagel G, et al. (2001) Interaction of cations, anions and weak base quinine with rat renal cation transporter rOCT2 compared with rOCT1. *Am J Physiol* **281:**F454–F468.

Bradford MM (1976) A rapid and sensitive method for the quantification of microgram quantities of protein utilizing the principle of protein-dye binding. *Anal Biochem* **72:**248–254.

Budiman T, Bamberg E, Koepsell H, and Nagel G (2000) Mechanism of electrogenic cation transport by the cloned organic cation transporter 2 from rat. *J Biol Chem* **275:**29413–29420.

Busch AE, Quester S, Ulzheimer JC, Waldegger S, Gorboulev V, Arndt P, Lang F, and Koepsell H (1996) Electrogenic properties and substrate specificity of the polyspecific rat cation transporter rOCT1. *J Biol Chem* **271:**32599–32604.

Dougherty DA (1996) Cation-π interactions in chemistry and biology: a new view of benzene, Phe, Tyr and Trp. *Science (Wash DC)* **271:**163–168.

Geering K, Theulaz I, Verrey F, Häuptle MT, and Rossier BC (1989) A role for the β-subunit in the expression of functional Na^+- K^+-ATPase in *Xenopus* oocytes. *Am J Physiol* **257:**C851–C858.

Gorboulev V, Shatskaya N, Volk C, and Koepsell H (2005) Subtype-specific affinity for corticosterone of rat organic cation transporters rOCT1 and rOCT2 depends on three amino acids within the substrate binding region. *Mol Pharmacol* **67:**1612–1619.

Gorboulev V, Ulzheimer JC, Akhoundova A, Ulzheimer-Teuber I, Karbach U, Quester S, Baumann C, Lang F, Busch AE, and Koepsell H (1997) Cloning and characterization of two human polyspecific organic cation transporters. *DNA Cell Biol* **16:**871–881.

Gorboulev V, Volk C, Arndt P, Akhoundova A, and Koepsell H (1999) Selectivity of the polyspecific cation transporter rOCT1 is changed by mutation of aspartate 475 to glutamate. *Mol Pharmacol* **56:**1254–1261.

Gründemann D, Gorboulev V, Gambaryan S, Veyhl M, and Koepsell H (1994) Drug excretion mediated by a new prototype of polyspecific transporter. *Nature (Lond)* **372:**549–552.

Gründemann D and Koepsell H (1994) Ethidium bromide staining during denaturation with glyoxal for sensitive detection of RNA in agarose gel electrophoresis. *Anal Biochem* **216:**459–461.

Hirai T, Heymann JAW, Shi D, Sarker R, Maloney PC, and Subramaniam S (2002) Three-dimensional structure of a bacterial oxalate transporter. *Nat Struct Biol* **9:**597–600.

Ho SN, Hunt HD, Horton RM, Pullen JK, and Pease LR (1989) Site-directed mutagenesis by overlap extension using the polymerase chain reaction. *Gene* **77:**51–59.

Huang Y, Lemieux MJ, Song J, Auer M, and Wang D-N (2003) Structure and mechanism of the glycerol-3-phosphate transporter from *Escherichia coli. Science (Wash DC)* **301:**616–620.

Koepsell H (2004) Polyspecific organic cation transporters: their functions and interactions with drugs. *Trends Pharmacol Sci* **25:**375–381.
Koepsell H and Endou H (2004) The SLC22 drug transporter family. *Pflueg Arch Eur J Physiol* **447:**666–676.
Koepsell H, Gorboulev V, and Arndt P (1999) Molecular pharmacology of organic cation transporters in kidney. *J Membr Biol* **167:**103–117.
Koepsell H, Schmitt BM, and Gorboulev V (2003) Organic cation transporters. *Rev Physiol Biochem Pharmacol* **150:**36–90.
Mehrens T, Lelleck S, Çetinkaya I, Knollmann M, Hohage H, Gorboulev V, Bokník P, Koepsell H, and Schlatter E (2000) The affinity of the organic cation transporter rOCT1 is increased by protein kinase C-dependent phosphorylation. *J Am Soc Nephrol* **11:**1216–1224.
Meyer-Wentrup F, Karbach U, Gorboulev V, Arndt P, and Koepsell H (1998) Membrane localization of the electrogenic cation transporter rOCT1 in rat liver. *Biochem Biophys Res Commun* **248:**673–678.
Valentin M, Kühlkamp T, Wagner K, Krohne G, Arndt P, Baumgarten K, Weber W-M, Segal A, Veyhl M, and Koepsell H (2000) The transport modifier RS1 is localized at the inner side of the plasma membrane and changes membrane capacitance. *Biochim Biophys Acta* **1468:**367–380.
Veyhl M, Spangenberg J, Püschel B, Poppe R, Dekel C, Fritzsch G, Haase W, and Koepsell H (1993) Cloning of a membrane-associated protein which modifies activity and properties of the Na^+-D-glucose cotransporter. *J Biol Chem* **268:**25041–25053.
Volk C, Gorboulev V, Budiman T, Nagel G, and Koepsell H (2003) Different affinities of inhibitors to the outwardly and inwardly directed substrate binding site of organic cation transporter 2. *Mol Pharmacol* **64:**1037–1047.
Wolff NA, Grünwald B, Friedrich B, Lang F, Godehardt S, and Burckhardt G (2001) Cationic amino acids involved in dicarboxylate binding of the flounder renal organic anion transporter. *J Am Soc Nephrol* **12:**2012–2018.
Yu EW, McDermott G, Zgurskaya HI, Nikaido H, and Koshland DE Jr (2003) Structural basis of multiple drug-binding capacity of the AcrB multidrug efflux pump. *Science (Wash DC)* **300:**976–980.

Address correspondence to: Dr. Hermann Koepsell, Institute of Anatomy and Cell Biology, Koellikerstr. 6, 97070 Würzburg, Germany. E-mail: hermann@koepsell.de